Cellular Signalling 63 (2019) 109382

Contents lists available at ScienceDirect

Cellular Signalling

journal homepage: www.elsevier.com/locate/cellsig

On the relationship of YAP and FAK in hMSCs and osteosarcoma cells: Discrimination of FAK modulation by nuclear YAP depletion or YAP silencing

Ayman Husari[b,c], Thorsten Steinberg[a,*], Martin Philipp Dieterle[a], Oswald Prucker[d], Jürgen Rühe[d], Britta Jung[b], Pascal Tomakidi[a]

[a] Division of Oral Biotechnology, Center for Dental Medicine, Medical Center - University of Freiburg, Faculty of Medicine, University of Freiburg, Hugstetter Str. 55, 79106 Freiburg, Germany
[b] Department of Orthodontics, Center for Dental Medicine, Medical Center - University of Freiburg, Faculty of Medicine, University of Freiburg, Hugstetter Str. 55, 79106 Freiburg, Germany
[c] Faculty of Engineering, University of Freiburg, Georges-Köhler-Allee 101, 79110 Freiburg, Germany
[d] IMTEK-Department of Microsystems Engineering, University of Freiburg, Georges-Köhler-Allee 101, 79110 Freiburg, Germany

ARTICLE INFO

Keywords:
Yes-associated protein (YAP) co-transcriptional activator
Focal adhesion kinase (FAK)
Focal adhesions (FAs)
Proliferation
Senescence
Osteogenic genes
Osteosarcoma cells (Saos)

ABSTRACT

The HIPPO pathway effector YAP has been shown to be regulated by FAK-signaling. However, the existence of an inverse relationship between YAP and FAK is unknown. Here we demonstrate in hMSCs and in the human osteosarcoma derived cell line Saos that Verteporfin- or RNAi-dependent YAP depletion has opposing influence on FAK. While Verteporfin strikingly reduced cellular FAK protein and phosphorylation, RNAi led to an increase of both molecules and point on a generalizable aspect of the YAP/FAK interrelationship. YAP depletion also caused down-regulation of osteogenic genes in hMSCs, irrespective from the YAP intervention mode. Verteporfin induced topological changes in conjunction with reduced protein levels of β1 integrin, paxillin, and zyxin of focal adhesions (FAs) in hMSCs, suggesting FAK-decrease-related alterations in FAs, which seems to be a FAK-dependent mechanism. On the cell behavioral level, YAP-FAK-interrelation involves proliferation and senescence, as indicated by proliferation inhibition and increase of β-Galactosidase-activity in hMSCs. Our findings, derived from this dual strategy of YAP intervention, reveal a YAP-FAK relationship in conjunction with molecular and cell behavioral consequences. Moreover, they deepen the current scientific knowledge on YAP from a different scientific point of view, since this inverse YAP/FAK-relationship seems to be transferrable to other cell types, including cell entities with pathological background.

1. Introduction

In conjunction with its homolog TAZ, the yes-associated protein (YAP) biologically functions as a co-transcriptional activator and both of them are part of the canonical HIPPO pathway [1]. As key elements of this pathway, they are indispensable for the cell-innate regulation of proliferation and differentiation, since nuclear YAP presence for instance protects cells from premature differentiation in vivo [2]. On the other hand, uncontrolled abundance of YAP in the nucleus can lead to tissue hyperplasia [3], and is also involved in the causation of cell transformation-based cancer development [4]. From the mechanistic viewpoint, YAP has to be present in the non-phosphorylated state to exert its biological function, since only this status permits the subcellular state of nuclear YAP localization [5]. The so far known portfolio of external cues which trigger nuclear topology of YAP are manifold and for instance include stimuli like mechanics and or biomechanics, increase in the number of cell-to-cell contacts, development of cell polarity, signaling and emerging from G protein-coupled receptors [2]. Though being integrated in the HIPPO pathway, latest findings decouple this state of nuclear YAP, since YAP entry into the nucleus for instance has been shown to be induced by force-triggered transport across nuclear pores, independent from LATS kinase action [6]. This translocation from YAP into the nucleus can be disabled by the photosensitizer Verteporfin (VP), through sequestration of YAP in the

* Corresponding author.
E-mail addresses: ayman.husari@uniklinik-freiburg.de (A. Husari), thorsten.steinberg@uniklinik-freiburg.de (T. Steinberg), stolldieterle@kabelbw.de (M.P. Dieterle), prucker@imtek.de (O. Prucker), ruehe@imtek.uni-freiburg.de (J. Rühe), britta.jung@uniklinik-freiburg.de (B. Jung), pascal.tomakidi@uniklinik-freiburg.de (P. Tomakidi).

https://doi.org/10.1016/j.cellsig.2019.109382
Received 17 April 2019; Received in revised form 30 July 2019; Accepted 30 July 2019
Available online 31 July 2019

cytoplasm, which is triggered through increased levels of 14–3-3σ. This molecule functions as a YAP chaperon protein that retains YAP in the cytoplasm and targets it for degradation in the proteasome ([7]). Such findings on HIPPO-independent nuclear YAP presence are not limited to in vitro experiments, employing cell cultures, but have also been discovered in vivo. Here, a direct link between integrin-FAK-derived signaling and YAP nuclear presence, under inclusion of the small RhoGTPase Cdc42 and the protein serine/threonine phosphatase PP1, as intermediate FAK-downstream signaling steps, has been recently described for stem cell-based tissue renewal in mice [2]. In this context it has been previously demonstrated that FAK is able to directly modulate Cdc42 activity [8], but also that cytoplasmic YAP is a positive regulator of this small GTPase [9].

The non-receptor tyrosine kinase FAK, essential for the establishment and turn-over of integrin-matrix-based cell adhesions has been reported to be involved as a signaling element in malignant tumor development, with emphasis on metastasis. In this context, RNA interference approaches, which specifically target (i) the serine/threonine kinase LKB1, acting as tumor suppressor, (ii) the multi-functional scaffold protein DIXDC1, and the microtubule affinity-regulating kinase MARK1, respectively, have been demonstrated to yield a FAK gain of function effect, which is substantiated by both a modulation of FAK on the protein as well as activation level [10,11]. Another facet of FAK silencing, which becomes apparent on the cell behavioral level in vitro, is the induction of senescence, as described for ras-transformed breast cancer cells [12]. In addition, other studies in carcinoma cells have shown that decrease in FAK activation, particularly addressing the p-FAK^{Tyr397} site, are sufficient as trigger of senescence [13].

In the present study, we employed hMSCs and osteosarcoma cells as an in vitro model system for investigating the stem cell-inherent and cancer cell-related molecular consequences of YAP depletion. We show that within the dual strategy approach chosen, pharmacological YAP intervention by VP, caused serious diminution of both FAK protein and activation at FAK^{pTYR397} and FAK ^{pTYR576} as well, and that YAP-RNAi triggers the opposite effect, i.e., increase in FAK protein and phosphorylation of the aforementioned FAK tyrosine residues. Further molecular consequences of YAP nuclear exclusion in hMSCs included down-modulation of the osteogenic genes collagen type I and osteopontin, and in case of VP-driven FAK depletion, topological changes in conjunction with reduced protein levels for ß1 integrin, paxillin, and zyxin of focal adhesions. The YAP-dependent findings on behalf of FAK, though of opposing nature, identify a so far unrecognized existence of an interrelationship between YAP and FAK, which, on the cell behavioral level becomes manifest by involving proliferation and senescence at least in hMSCs.

2. Materials and methods

2.1. Cells

hMSCs (Promocell, Germany) were used at passage 3 for all experiments and cultivated in StemMACS MSC Expansion Medium human, containing 10% Cytomix (Miltenyi Biotec GmbH, Germany). Saos-2 cells were obtained from (ATCC, Wesel, Germany) (passage 6) were grown in Dulbecco's Modified Eagle Medium (DMEM, Thermo Fisher Scientific, Germany) supplemented 2 mM L-alanyl-L-glutamin (Thermo Fisher Scientific), 0.1 mg/ml Kanamycin (Sigma-Aldrich, Germany) and 10% fetal calf serum (FCS, Biochrom, Germany). All Cells were incubated at 37 °C and 5% CO_2.

2.2. Inhibitior treatment by Verteporfin

To evaluate the best effect of VP (Sigma Aldrich) with respect to nuclear YAP exclusion, hMSCs were exposed to three different concentrations, namely 1 μM, 3 μM and 5 μM. In the experimental setup, hMSCs and SaOs cells were cultivated for 24 h prior to 72 h VP incubation.

2.3. siRNA transfection

The set of 2 different Silencer Select YAP-SiRNAs (Si YAP-1 ID20366 and ID20368) and 2 different Silencer PTK2-SiRNAs (Si PTK2 ID103649 and ID103698) were purchased from (Thermo Fisher Scientific), to exclude off-target effects. After 48 h, MSC Medium was replaced by DMEM without serum and antibiotics, and the siRNA transfection was performed with a final concentration of 30 pmol/ml, using lipofectamine RNAiMAX (Thermo Fisher Scientific) as transfection reagent. hMSCs or Saos cells were incubated with siRNA for 72 h.

2.4. Inhibitior treatment by FAK inhibitor 14 (Y15)

FAK inhibitor 14, (1,2,4,5-Benzenetetraamine tetrahydrochloride) or (Y15) was ordered from (Sigma Aldrich) and used at concentration of 5 μM to test the effect of FAK inhibition. hMSCs were incubated with Y15 for 72 h.

2.5. Primary antibodies

For Indirect Immunofluorescence (IIF) and Western blot (WB) analyses, primary antibodies against yes-associated protein (YAP; mouse monoclonal, sc-376,830, Santa Cruz, Germany), focal adhesion kinase (FAK; rabbit monoclonal, ab76496, Abcam, UK), the phospho specific focal adhesion kinase pFAK Tyr-397 (rabbit monoclonal, ab81298, Abcam), the focal adhesion kinase phosphorylated at Tyr-576 (rabbit monoclonal, ab76244, Abcam), 14–3-3 Sigma (mouse monoclonal, ab14123, Abcam), ß1-Integrin (mouse monoclonal, sc-374,429, Santa Cruz), Paxillin (mouse monoclonal, MA5–13356, Thermo Fisher Scientific), Osteopontin (mouse monoclonal, ab69498, Abcam), zyxin (mouse monoclonal, ab58210, Abcam), collagen1α1 (C2456, SigmaAldrich) and GAPDH (mouse monoclonal,sc-365,062, Santa Cruz) were used.

2.6. Indirect Immunofluorescence (IIF)

Using the above-mentioned primary antibodies, IIF was performed as described by [14]. In brief, specimens were washed with PBS, fixed with 3.8% paraformaldehyde solution, and permeabilized with blocking solution. Thereafter, specimens were incubated with primary antibodies. Then, samples were incubated with secondary antibodies AlexaFluor594 (goat anti-mouse or anti-rabbit, Thermo Fisher Scientific). For actin cytoskeleton staining, specimens were incubated with Phalloidin-Alex488 (Thermo fisher scientific). Nuclear staining was performed with DAPI (Thermo fisher scientific). Finally, samples were embedded in mounting medium fluoromount G (Biozol Diagnostica, Germany). IIF was visualized with the Keyence BZ-9000 fluorescence microscope (KEYENCE GmbH, Neu-Isenburg, Germany).

2.7. Western blot analysis

After 72 h incubation of hMSCs or SaOs cells either with VP, siRNA or Y15, whole cell lysates were used. To obtain whole cell lysate cells were washed with PBS and incubated for 5 min in 200 μl RIPA buffer (Sigma-Aldrich) supplemented with cOmplete Mini Protease Inhibitor Cocktail (Thermo fisher scientific) and PhosSTOP phosphatase inhibitor (Sigma-Aldrich) on ice. Subsequently, lysates were collected and centrifuged for 10 min at 10.000 rpm 4 °C. The supernatants were used for total protein amount measurement using Pierce BCA Protein Assay Kit (Thermo fisher scientific). Nuclear fractions and Cytoplasmic fractions were generated by employing the subcellular Protein Fractionation Kit (Thermo fisher Scientific). For each blot, 5 μg–10 μg of total protein depending on the biomarker under investigation was separated by SDS-PAGE on 4–15% Criterion TGX Stain-Free precast gels (Bio-Rad,

Germany). Proteins were transferred to low-fluorescence PVDF membranes (Bio-Rad, USA). After blocking with Tris-buffered saline TBS (Bio-Rad), containing 0.2% Tween20 (Bio-Rad) and 5% bovine serum albumin BSA for 2 h at room temperature (RT), membranes were incubated overnight at 4 °C with primary antibodies YAP, FAK, FAK-Y397, FAK-Y576, Zyxin and GAPDH (wd 1:5000), Osteopontin and 14–3-3 Sigma (wd 1:1000), Paxillin and ß1-Integrin (wd 1:500) in TBS-Tween20, containing 0.5% BSA. Subsequently, membranes were incubated with horseradish peroxidase-labeled secondary antibody (wd 1:5000) (Li-Cor Biosciences, USA) for 1 h at RT. Membranes were imaged for total protein quantification with the stain free application method of the ChemiDoc Touch imager, allowing the omission of house-keeping protein [15]. The proteins of interest were detected, using the Clarity Western ECL Blotting Substrate (Bio-Rad, Germany) and chemiluminescence application of the ChemiDoc Touch imager (Bio-Rad, Germany. The protein bands were normalized to total protein level in the respective lane and subsequently to the untreated control with ImageLab software (version 5.2.1; Bio-Rad). The protein bands were normalized to total protein level in the respective lane and subsequently to the untreated control with ImageLab software (version 5.2.1; Bio-Rad). For quantification and graphical documentation, this untreated control was set to 100% pixel density and used as reference value for comparison with bands of treated samples.

2.8. RNA isolation and quantitative real-time PCR

The relative gene expression of bone-specific markers collagen type I alpha 1 (COL1α1, RefSeq# NM_000088), Osteopontin (SPP1) (NM_000582) and Protein tyrosine kinase 2 (PTK2) (NM_001199649) assessed on mRNA level by semi quantitative real-time RT-PCR.

After 72 h hMSCs culture period either with VP orsiRNA, the total RNA was isolated from hMSCs, using the RNeasy plus mini kit (Qiagen, Germany). RNA concentration and integrity was measured by a QIAxpert instrument (Qiagen). Synthesis of cDNA was performed with 100 ng mRNA using RevertAid First Strand cDNA Synthesis Kit (Thermo Fisher Scientific) according to the manufacturer's protocol using a C1000 Thermal Cycler (Bio-Rad). Real-time PCR reactions were carried out with the CFX96- Real-Time PCR Detection System (Bio-Rad Laboratories) using RT^2 SYBR Green qPCR Master Mix from (Qiagen), and cDNA equivalent to 10 ng of total mRNA. 1 µl pre-dispensed gene-specific primer pairs were pipetted into each well containing 24 µl of the master mix. Relative mRNA expression of COL1A1, SPP1 and PTK2 was normalized to the housekeeping genes ribosomal protein RPL13a (RPL13A; RefSeq# NM_012423, Qiagen), Ubiquitin C (UBC; RefSeq# NM_021009, Qiagen) and glyceraldehyde-3-phosphate dehydrogenase (GAPDH; RefSeq# NM_001256799, Qiagen). Data were collected and analyzed using CFX96 Manager Software version 1.0 (Bio-Rad).

2.9. Real time cell analysis (RTCA) system (iCelligence)

The iCelligence instrument (OLS OMNI Life Science, Germany) was used to monitor in real-time the cell proliferation of hMSCs. To measure the blank of the impedance, 100 µl of culture medium was added to each well of the 8-well electronic microtiter plate (OLS OMNI Life Science). Next, 5×10^3 cells per 500 µl culture medium were seeded in each well. After cells were attached to the bottom of the plate which is covered with gold micro electrodes and sensors, the plate was placed into the incubator at 37 °C and 5% CO_2 and the proliferation was monitored using RTCA system. VP was added after 24 h. After 48 h siRNA was added after the MSC Medium was replaced with Dulbecco's Modified Eagle Medium (DMEM; Thermo Fisher Scientific) without serum and antibiotic. Cell index (density) was measured every 5 min up to 120 h. Data were analyzed using RTCA software (version 1.0 OLS).

2.10. β-Galactosidase staining

Senescence-associated-ß-galactosidase (SA-ß-gal) activity was determined using a Cellular Senescence Assay Kit (Merck Millipore, Germany), according to manufacturer's instructions. Briefly, hMSCs were washed twice with PBS and fixed with 4% paraformaldehyde and 0.1% glutaraldehyde. Then the fixing solution was removed and hMSCs were washed. SA-ß-gal detection solution was added and hMSCs were incubated at 37 °C without CO_2 at the dark overnight. Senescent cells were identified as blue-stained cells by standard light microscopy. 300 cells were counted in random fields to determine the percentage of SA-ß-gal positive cells.

2.11. Statistical analysis

All experiments were performed in at least 3 biological replicates. All data are expressed as mean ± standard error (SEM). GraphPad software (version 6, La Jolla, USA) was used to perform statistical tests. Differences were analyzed using one-way ANOVA and meant *t*-test comparisons between all groups and were considered significant when ($p < .05$).

3. Results

3.1. Verteporfin depletes nuclear YAP and affects FAK in hMSCs

To test our hypothesis on the putative interrelationship between YAP nuclear localization and FAK, we first exposed hMSC cultures to various concentrations of the photosensitizer VP, shown to reliably inhibit YAP nuclear presence [7,16]. Among the applied concentrations, 5 µM VP significantly depletes the amount of nuclear YAP to about 70% compared with non-treated control, as shown for hMSC nuclear protein extracts (Fig. 1, C and D).

VP-induced inhibition of nuclear YAP abundance was confirmed by IIF. Here, inhibitor-treated hMSCs showed blue nuclear DAPI-signals, while controls exhibited magenta nuclei through merger of red YAP and blue DAPI fluorescence (Fig. 1A). To determine the molecular consequences of YAP nuclear exclusion, we first focused on FAK, because of the already published work on YAP regulation through FAK signaling [2]. To this end, hMSC-derived total cell extracts, for the detection of FAs-molecules (Fig. 1 E), together with nuclear /cytoplasmic extracts (Fig. 1C), for testing the efficiency of nuclear YAP depletion on the one hand side and cytoplasmic accumulation at the same time on the other side, were subjected to WB analysis. In this context, the mechanistically involved YAP chaperon 14–3-3 protein revealed increasing amount with rising VP concentrations (Fig. 1C). At the same time, VP administration of 3 and 5 µM revealed almost equal efficacy, regarding prevention of YAP nuclear localization (Fig. 1C and D). Unexpectedly, total protein extracts (Fig. 1E) as well as cultured hMSCs analyzed by IIF (Fig. 1A) were almost completely devoid of FAK protein. Based on this finding, we analyzed subsequently, whether VP-induced lack of FAK, also holds true for FAK acting as key element in mechano-transduction [17,18]. Therefore, we probed membranes with antibodies, specifically detecting the autophosphorylation site at FAK tyrosine 397, and FAK kinase activity-indicating tyrosine residue 576. In both cases, the resulting protein bands were only weak, when compared to controls, thereby pointing to low activity at the analyzed tyrosine phosphorylation sites, i.e. FAK ^{pTYR397}, and FAK ^{pTYR576} (Fig. 1E), respectively. Reliability of the effects of VP on FAK was obtained from almost equal GAPDH levels in VP-treated cells (Fig. 1E). For both FAK tyrosine phosphorylation sites, the findings, obtained by WB could be corroborated by fluorescence detection. In case of FAK ^{pTYR397}, typical footprint-like patterns in controls were opposed by an inhibitor-related sparse cytoplasmic fluorescence (Fig. 1A), and for FAK ^{pTYR576}, the grain like red fluorescence of controls (Fig. 1A) was almost vanished in the presence of VP (Fig. 1A). These data suggest that VP-mediated

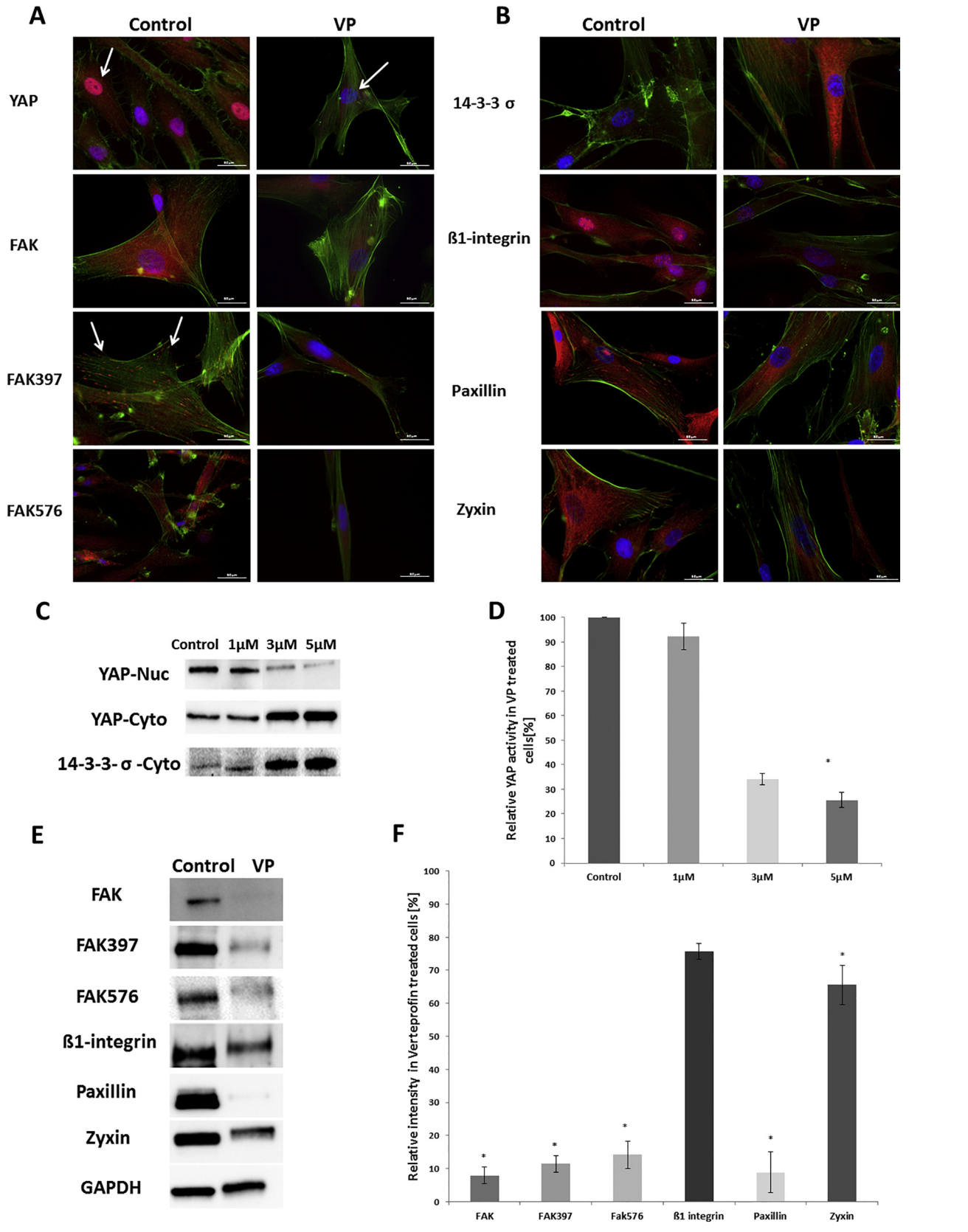

(caption on next page)

nuclear depletion of YAP addresses both, the cell-innate FAK protein content, but also FAK activity, which is required for mechano-transduction. If the inhibitor-mediated impact on FAK addresses focal adhesions (FAs), VP-treated hMSCs should exhibit different topological patterns and potentially reduced protein amounts of adhesion constituents, compared to their non-treated counterparts. To address this

Fig. 1. Verteporfin (VP) leads to: depletion of nuclear YAP, decrease of FAK, and alterations of FAs constituents.
(A and B) Indirect Immunofluorescence (IIF) shows YAP (see white arrows), FAK, FAK397(see white arrows), FAK576, 14–3-3, ß1 Integrin, Paxillin and Zyxin (red), Phalloidin-AlexaFluor488 staining for actin (green), and DAPI counter stain for cell nuclei (blue) of control and VP-treated hMSCs. Bars correspond to 60 μm. (C) Protein expression of YAP fraction (Nucleus and Cytoplasm) and cytoplasmic fraction of 14–3-3-σ analyzed in hMSCs after treatment with three different concentrations of VP (1 μM, 3 μM and 5 μM) detected by WB. Subsequent experiments were done with (5 μM). (D) YAP activity in VP-treated hMSC. The columns show that the YAP amount decreased in nuclear fraction with increasing VP concentration. (E and F) After 24 h cultivation, hMSCs were incubated with 5 μM for 72 h, the expression level of FAK, FAK397, FAK576, ß1 Integrin, Paxillin, Zyxin and GAPDH analyzed in whole cells extracts of VP-treated hMSCs and analyzed by WB. Bands were normalized to total protein level in the respective lane and subsequently to the untreated control with ImageLab software. Data represent 3 individual experiments (n = 3 ± SEM, *p < .05).

presumption, we performed IIF and WB for ß1 integrin, paxillin and zyxin, known to be essential FAs constituents [19]. Noticeable differences regarding the aforementioned molecules were detectable between the two groups with respect to both, their topology and quantity as well (Fig. 1, B and E).

With matched controls, hMSCs exhibited a declined fluorescence of ß1 integrin in response to the inhibitor, together with a reduced fluorescence stretching to cell borders for paxillin, which appeared even more pronounced for zyxin (Fig. 1B). These topological differences were mirrored by differential protein amounts, which were slightly reduced by the inhibitor in case of ß1 (approx.15%), medium for zyxin (approx. 30%), and substantially in the case of paxillin (approx. 90%), (Fig. 1, E and F). Interestingly, YAP RNAi only led to marginal changes of the assessed FAs components, regarding their topology and their protein quantity as well (Fig. 2, B-D). While YAP intervention via RNAi suggests unchanged FAs, the discriminative distribution and quantity of FAs constituents in VP-treated versus non-treated cells points to differences in the molecular architecture of FAs. To clarify, if the observed effects are a direct consequence of YAP-inhibition or probably FAK-dependent, we conducted the dual inhibition mode of action on hMSCs and analyzed the above-mentioned downstream/upstream molecular targets by IIF and WB analysis (Fig. 3). Interestingly, the results revealed a direct correlation between FAK-inhibition, independent from the inhibition mode of action (Fig. 3A and B), but significantly pronounced, if the siRNA-FAK approach was used (Fig. 3B).

3.2. YAP-specific siRNA depletes YAP though increasing FAK protein

To investigate, whether the down-modulation of FAK and its phosphorylation by pharmacological YAP exclusion from the nucleus is a basic and thus a generalizable effect, or VP-specific, we additionally conducted experiments on YAP depletion, by employing RNAi, directed against YAP. With matched controls, a combination of two YAP-specific siRNAs resulted in a striking decrease of YAP by approximately 80% in hMSC-derived protein extracts (Fig. 2, C and D). Specificity of the siRNA approach was confirmed by GAPDH detection, which showed clearly reduced levels in case of a GAPDH-specific siRNA (Fig. 2C), which was used as internal experimental control. SiRNA-induced decline of YAP was also seen in hMSCs, prepared for IIF, since control cells exhibited magenta and thus nuclear YAP fluorescence (Fig. 2A). Intriguingly, unlike the inhibitor, YAP RNAi yielded significant increased levels of total FAK protein in hMSC. When compared to controls, this finding was indicated by increased red-fluorescent dots within the entire cytoplasm (Fig. 2A), and confirmed by WB analysis (Fig. 2C). This increase was not restricted to the FAK protein, but also applied to the phosphorylation sites under study, i.e. the tyrosine residues $FAK^{pTYR397}$, and $FAK^{pTYR576}$ as well. In this context, these findings were reflected by detection of significant higher protein band intensities in WB (Fig. 2, C and D), and, in case of IIF, through a clear footprint-patterned $FAK^{pTYR397}$ red fluorescence signal in siRNA-treated cells, which was counteracted by a preferential cytoplasmic signal in controls (Fig. 2A). In case of $FAK^{pTYR576}$ higher WB-detected protein levels (Fig. 2, C and D) were coinciding with its elevated cytoplasmic fluorescence (Fig. 2A). These observations are in contrast with the inhibitor-related findings, and point to a positive regulation of FAK with respect to both, the protein amount and its activation, in case of YAP interference at the transcriptional level. Moreover, the diametrical FAK-pertaining findings, elaborated by the different inhibition modes of preventing YAP nuclear localization, may give a hint for the existence of a YAP-FAK-interrelationship. Regarding intergrin ß1, zyxin and paxillin protein distribution in siRNA-treated hMSCs detected by IIF (Fig. 2B) and the corresponding WB analysis (Fig. 2C), the protein levels remained almost unaffected.

To verify, if the above-mentioned diametrical FAK-related findings are perhaps generalizable and can be found in other cell types in which the interplay of YAP depletion on FAK is of particular interest, we performed the same experimental setup, which we used for hMSCs, for Saos cells. Interestingly, the results with the different inhibitory modes of action showed nearly the same trend in Saos cells as we have found before in hMSCs (Fig. 4). In detail, IIF of Saos cells showed the same inverse effect following Verterporfin or YAP siRNA treatment regarding the influence on the YAP upstream target FAK and the active forms FAK397, FAK576 (Fig. 4A and B) and could be confirmed on the protein level by WB analysis (Fig. 4C and D). Hence, the data point at a generalizable mechanism in cells of pathological and non-pathological origin.

3.3. YAP depletion modulates FAK transcription and osteogenic genes in hMSCs

Since hMSCs adopt different phenotypes in response to substrate stiffness [20], the stiffness of the conventional cell culture substrates of this study triggers their osteogenic phenotype. We therefore detected mRNA synthesis of FAK, together with the osteogenic indicators collagen type I (COL1A1) and osteopontin (SPP1) [21,22], to facilitate the identification of putative molecular consequences of the distinct ways of YAP intervention, particularly in light of the opposing outcome, regarding FAK (PTK2).

Following inhibitor administration, hMSCs were almost devoid of detectable PTK2 transcripts (Fig. 5D). In marked contrast, a vice versa situation could be denoted, when hMSCs were subjected to YAP RNAi. Here, hMSCs showed significantly elevated PTK2 transcription (Fig. 5H). This inverse situation, detected on the transcriptional level, parallels the findings of the FAK protein patterns described above, thereby pointing to a regulatory effect of YAP on FAK, and further evidencing the YAP-FAK-interrelation. For the osteogenic genes COL1A and SPP1, the results were notable, since both biomarkers showed, although not significant, decreased transcription, regardless of the chosen YAP intervention mode (Fig. 5, D and H).

Concerning a putative biological impact of YAP intervention, this concordance in down-modulation of transcription may be a hint that COL1A1 and SPP1 mRNA synthesis may be governed by YAP, rather than the approach of YAP intervention per se. In case of a possible transcriptional regulation of the assessed osteogenic markers through nuclear YAP, the down-modulated transcription should be mirrored by corresponding protein patterns. For both molecules, a clear reduction of the grain-like red IIF-fluorescence signal, decorating perinuclear sites and stretching in adjacent cytoplasmic regions was seen, when hMSCs were treated with VP and YAP-specific siRNA, respectively (Fig. 5, A and E). This suggests that the impact of YAP depletion becomes manifest also on the protein level, thereby pointing to veritable YAP interventional molecular consequences in hMSCs. To scrutinize this

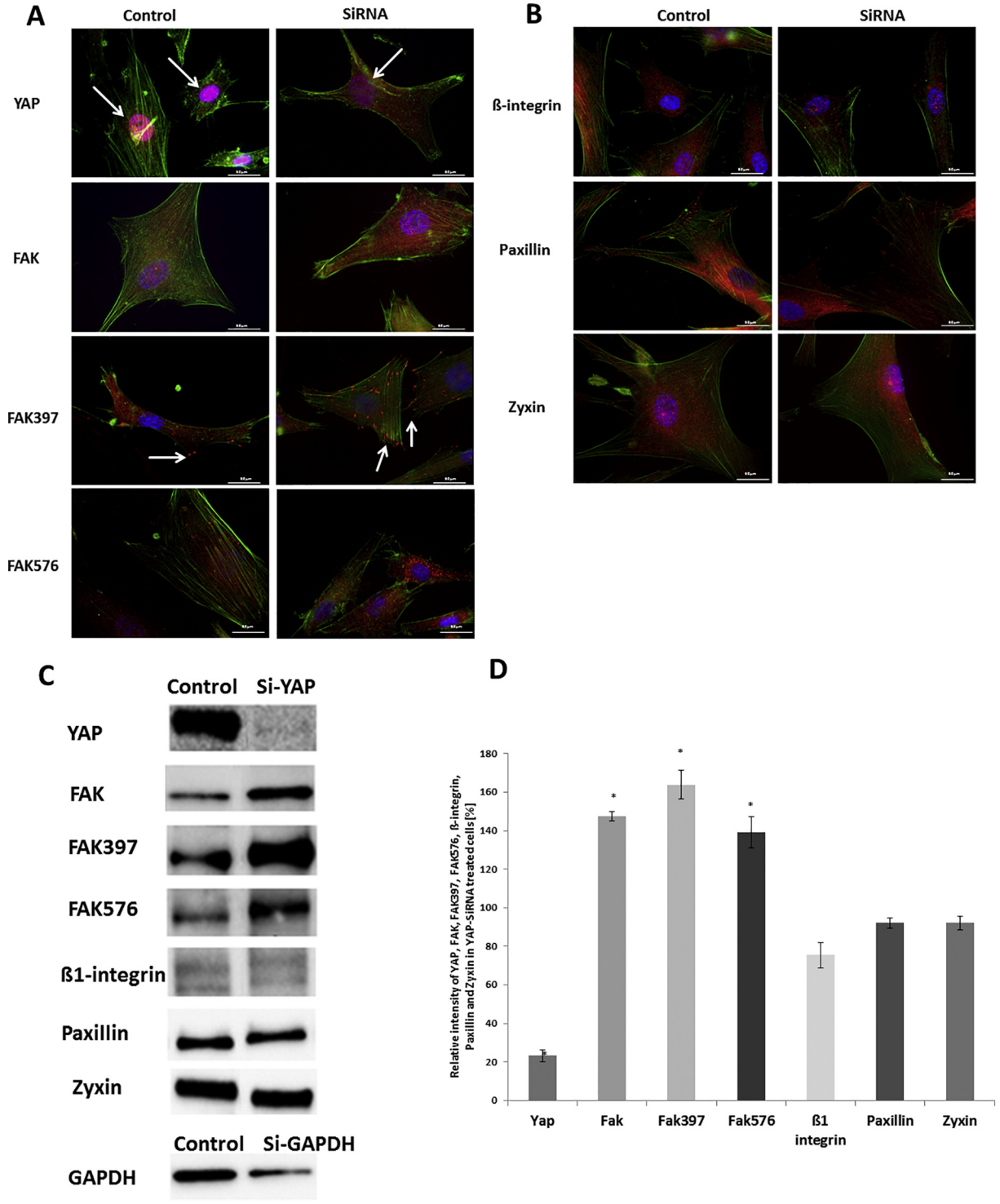

Fig. 2. YAP-RNAi declines YAP and increases FAK, while FAs constituents remain fairly unchanged.
(A and B) Indirect Immunofluorescence (IIF) shows YAP (see white arrows), FAK, FAK397 (see white arrows), FAK576, ß1 Integrin, Paxillin and Zyxin (red), Phalloidin-AlexaFluor488 staining for actin (green), and DAPI counter stain for cell nuclei (blue) of control and YAP-RNAi- treated hMSCs. Bars correspond to 60 µm. (C and D) Protein expression of YAP, FAK, FAK397, FAK576, ß1 Integrin, Paxillin and Zyxin analyzed after treatment of hMSCs with YAP-RNAi for 72 h detected by WB. As internal experimental control, RNAi against GAPDH yielded decreased protein levels. Bands were normalized to total protein level in the respective lane and subsequently to the negative control with ImageLab software. Data represent 3 individual experiments ($n = 3 \pm SEM$, $^*p < .05$).

aspect, we conducted WB, followed by specific antigen detection. As exemplified for osteopontin, total cell extracts revealed significant lower SPP1 protein amounts in VP-derived hMSC extracts (Fig. 5, B and C), a pattern, which also applied, although not to the same significant extend, to extracts obtained by RNAi (Fig. 5, F and G). This coincidence of reduced mRNA levels and protein expression, detected for SPP1, emphasizes the notion of YAP depletion-related molecular consequences, which may presumably be governed by YAP's biological function in acting as a nuclear co-transcription activator.

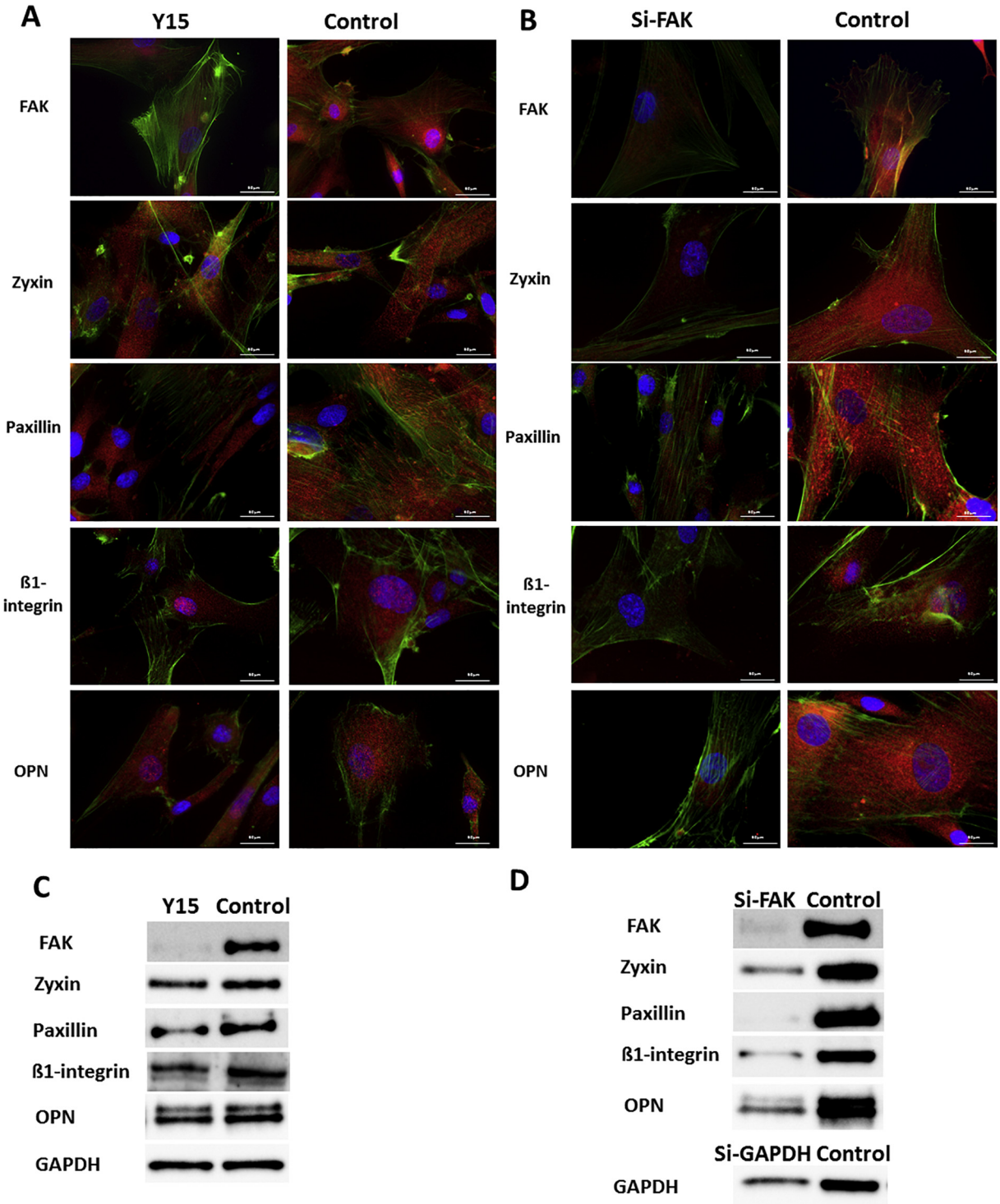

Fig. 3. The effect of FAK-inhibitor 14 (Y15) and FAK-SiRNA in hMSC cells. (A) Indirect Immunofluorescence (IIF) of Y15- and (B) FAK-RNAi- treated hMSCs. FAK, Zyxin, Paxillin, ß1-integrin and OPN (red), Phalloidin-AlexaFluor488 staining for actin (green), and DAPI counter stain for cell nuclei (blue). Bars correspond to 60 µm. (C) Protein expression of FAK, Zyxin, Paxillin, ß1-integrin and OPN in Y15- and (D) in FAK-RNAi-treated hMSCs detected by WB. Bands were normalized to total protein level in the respective lane and subsequently to the untreated control with ImageLab software. Exemplified representative illustrations of 3 individual experiments. (For interpretation of the references to colour in this figure legend, the reader is referred to the web version of this article.)

3.4. Differential impact of YAP-FAK interrelationship on cell behavior is determined by the YAP intervention mode

It is frequently reported that the biological function of YAP as a co-transcriptional activator results in the promotion of cell behavioral features, such as proliferation [23]. Therefore, we were next interested in looking for putative consequences on hMSC proliferation within the YAP-FAK-interrelationship, which may emerge from YAP depletion. To this end, we conducted impedance measurement-based real-time monitoring of hMSC proliferation either in the presence of the inhibitor VP or the YAP-specific siRNA. The respective cell indices revealed an impact on proliferation, irrespective from the modus operandi, chosen for nuclear YAP intervention (Fig. 6, A and B). Although the severity of proliferation attenuation is fairly comparable at the end of the

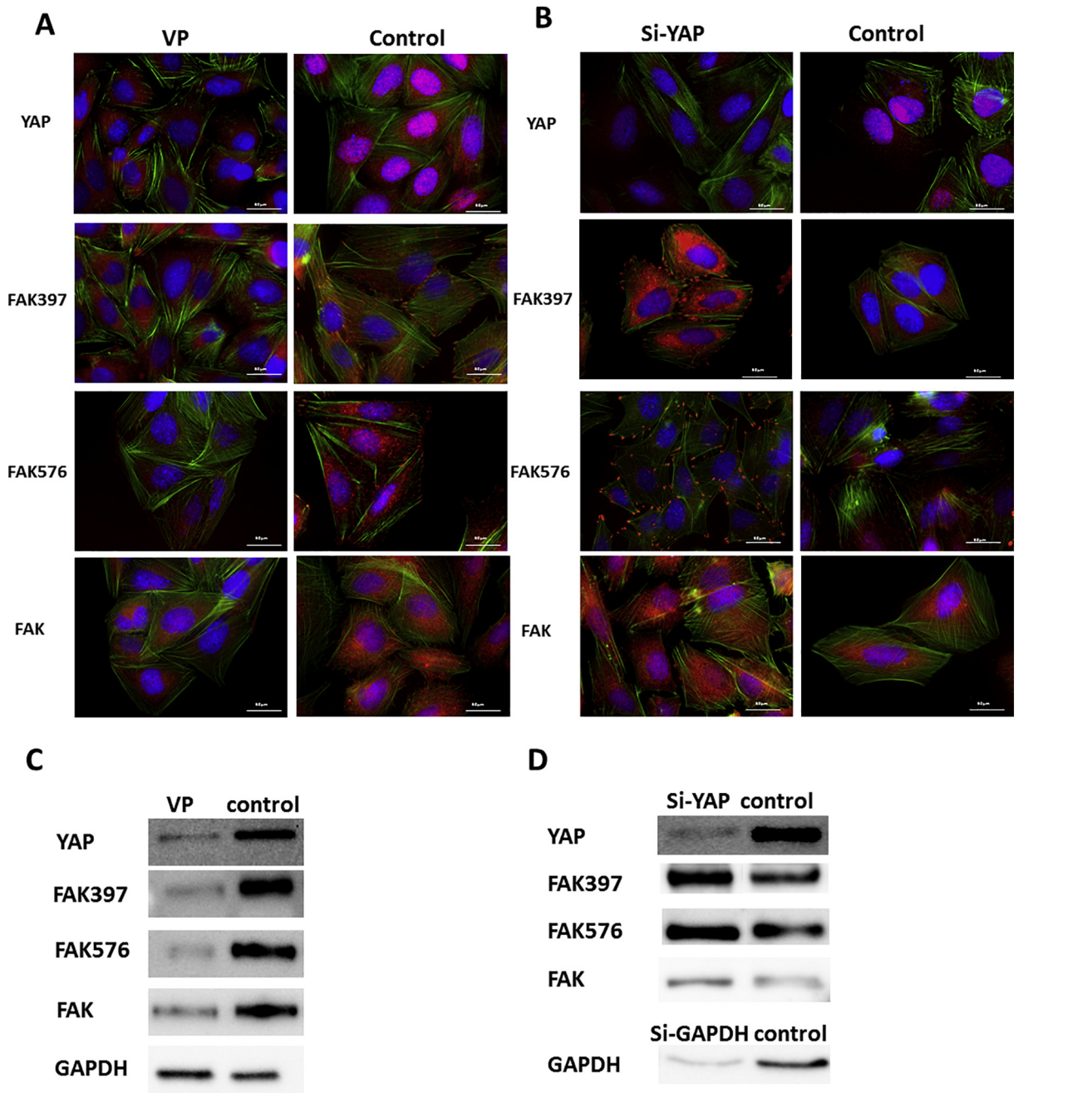

Fig. 4. The effect of VP and YAP-SiRNA in Saos cells. (A) Indirect Immunofluorescence (IIF) of VP-treated hMSCs and (B) of YAP-RNAi- treated hMSCs. YAP, FAK397, FAK576 and FAK (red), Phalloidin-AlexaFluor488 staining for actin (green), and DAPI counter stain for cell nuclei (blue). Bars correspond to 60 μm. (C) Protein expression of YAP, FAK397, FAK576, and FAK in VP-treated hMSCs and (D) inYAP-RNAi- treated hMSCs analyzed and detected by WB. Bands were normalized to total protein level in the respective lane and subsequently to the untreated control with ImageLab software. Exemplified representative illustrations of 3 individual experiments. (For interpretation of the references to colour in this figure legend, the reader is referred to the web version of this article.)

respective observation periods, in both cases cell indices of approximately 0.8–0.9 were detected (compare Fig. 6, A and B), the duration of reaching this cell indices between treated and non-treated controls differed between the inhibitor and the RNAi approach. This was substantiated by the time periods when the index curves started to separate up till reaching their maximum difference.

While therefore approximately 85 h could be denoted in hMSC cultures treated with the inhibitor (Fig. 6A), only about 60 h were detected for cells exposed to YAP-specific siRNA (Fig. 6B). These results suggest that YAP depletion in general affects cell behavioral proliferation, i.e. regardless of preventing nuclear presence via inhibitor intervention or its cellular protein availability per se through RNAi. Moreover, they point to operation mode-dependent differences in the efficacy of manifestation with respect to the time scale.

One of the novel findings in the present study, which adds to the body of evidence of a YAP-FAK interrelation, is the VP-related depletion of FAK. It has been described that with respect to FAK, FAK silencing or decrease in FAK activity was associated with cell senescence [12,13], which, on the cell behavioral level, finally entails cessation of cell growth [24]. Therefore, we analyzed this cell behavioral feature in our hMSCs in response to YAP intervention. By counting the number of ß-galactosidase activity (ß-Gal) exhibiting cells, VP administration yielded significantly higher numbers, nearly 15%, of ß-Gal-positive cells with matched controls (Fig. 6, C and D). In contrast, cultures

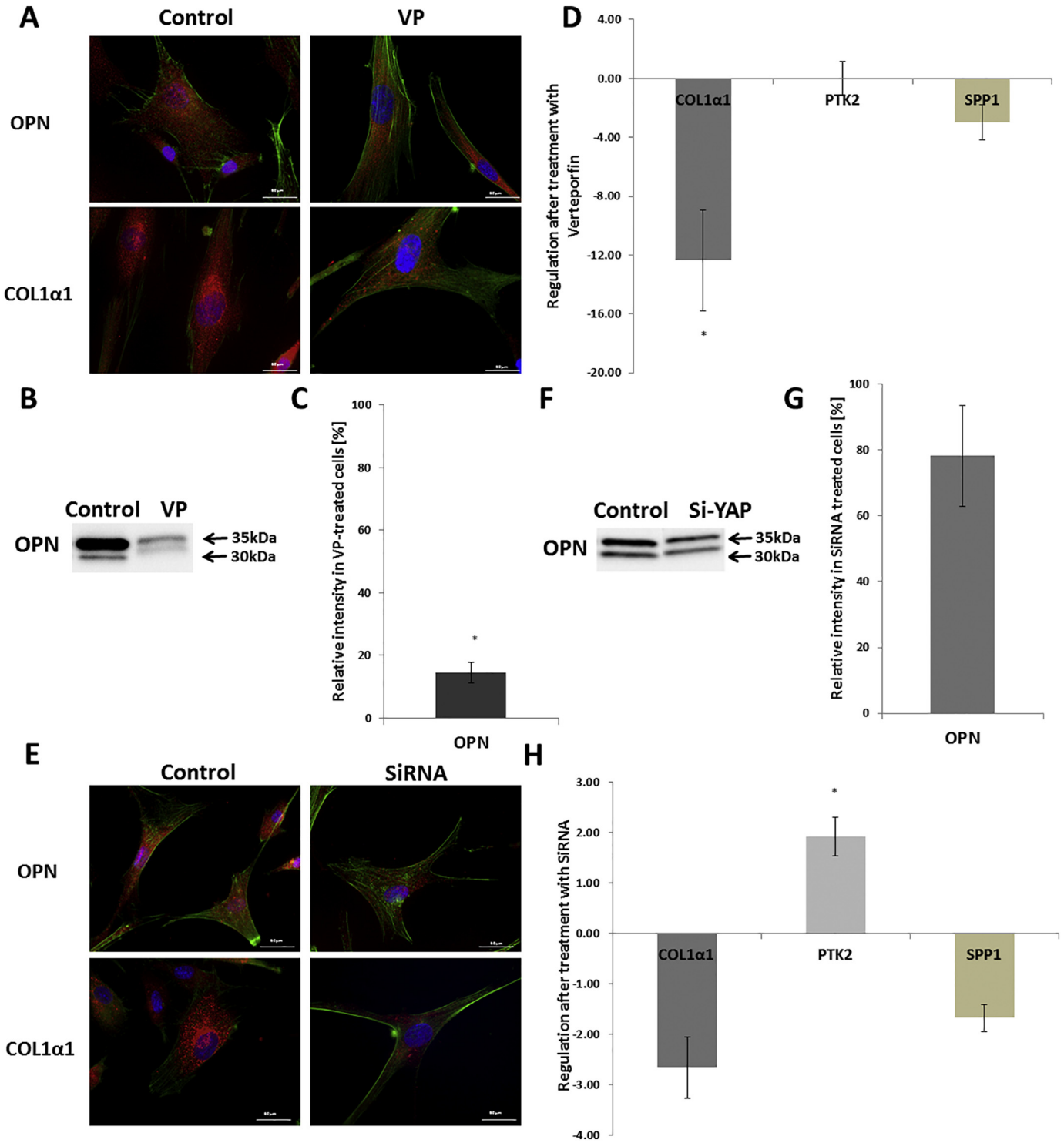

Fig. 5. YAP intervention generally causes down-regulation of osteogenic genes. (A and E) Indirect Immunofluorescenc (IIF) shows OPN and COL1α1 (red), Phalloidin-AlexaFluor488 staining for actin (green), and DAPI counter stain for cell nuclei (blue) of VP-and YAP-RNAi- treated hMSCs, respectively. (B, C and F, G) Western Blot analysis of OPN after treatment of hMSCs with VP and YAP-RNAi, respectively. (D and H) Regulation of COL1α1, PTK2 and SPP1 gene transcription of treated hMSCs with VP or SiRNA for 72 h, respectively. Data represent 3 individual experiments (n = 3 ± SEM, *p < .05). (For interpretation of the references to colour in this figure legend, the reader is referred to the web version of this article.)

exposed to siRNA responded with an only marginal increase of about 3%, compared to untreated counterparts (Fig. 6, E and F). These ß-Gal-patterns may suggest that YAP intervention may per se influence hMSC-senescence, but that the extent of cell senescence may depend on the protein and activation status of FAK. The major findings obtained from YAP intervention by either employing VP or RNAi, respectively, are illustrated in Fig. 7.

4. Discussion

With respect to YAP activity, there is accumulating evidence that it is controlled by pathways other than HIPPO, as recently described for

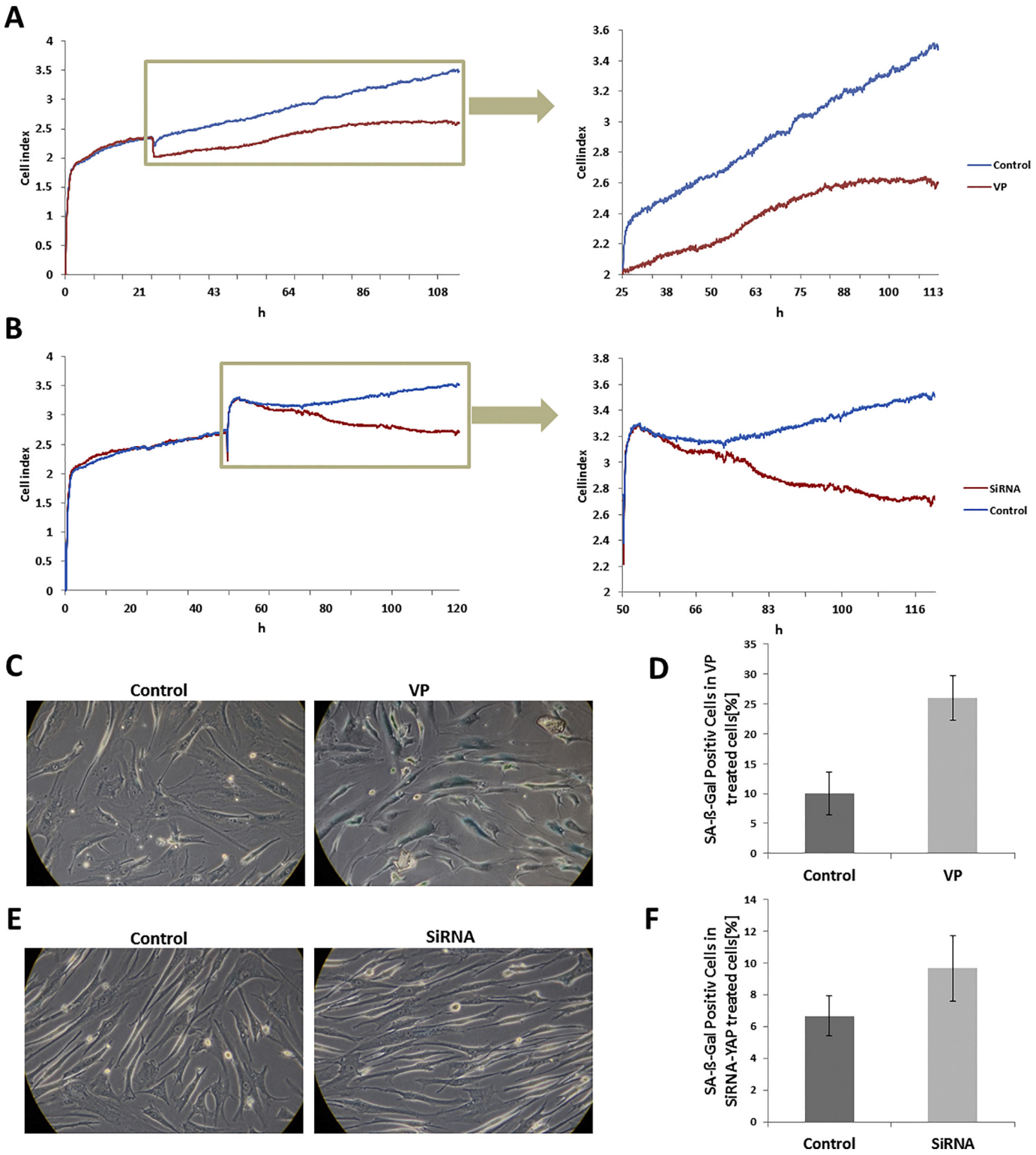

Fig. 6. YAP depletion influences cell behavior in hMSC, i.e. proliferation and senescence. **(**A and B**)** Illustrate the effect of VP and YAP-RNAi on hMSC proliferation detected by impedance measurement. Cells were seeded in *E*-plates L8. Cell index was calculated by impedance measurement every 5 min up to 120 h. VP was added after 24 h. MSC Medium was replaced with Dulbecco's Modified Eagle Medium (DMEM) without Serum and Antibiotic then the SiRNA was added after 48 h. **(**C, D and E, F**)** show the SA-ß-gal positive cells in VP- and YAP-RNAi- treated hMSCs, respectively. Senescent cells were identified as blue-stained cells by standard light microscopy. Percentages of the SA-ß-gal positive cells were quantified by counting a total of 300 cells in random fields. Data represent 3 individual experiments (n = 3 ± SEM, *p < .05). (For interpretation of the references to colour in this figure legend, the reader is referred to the web version of this article.)

integrin-FAK-signaling [2]. Although hereby YAP has been identified as an integrin-FAK down-stream target, a possible relationship between YAP and YAP-related up-stream signaling events has still to be elucidated. Regarding molecular constituents of such up-stream events, we first-time show in this study that YAP mechanistically acts as a FAK modulator, depending on the mode of YAP intervention. Co-

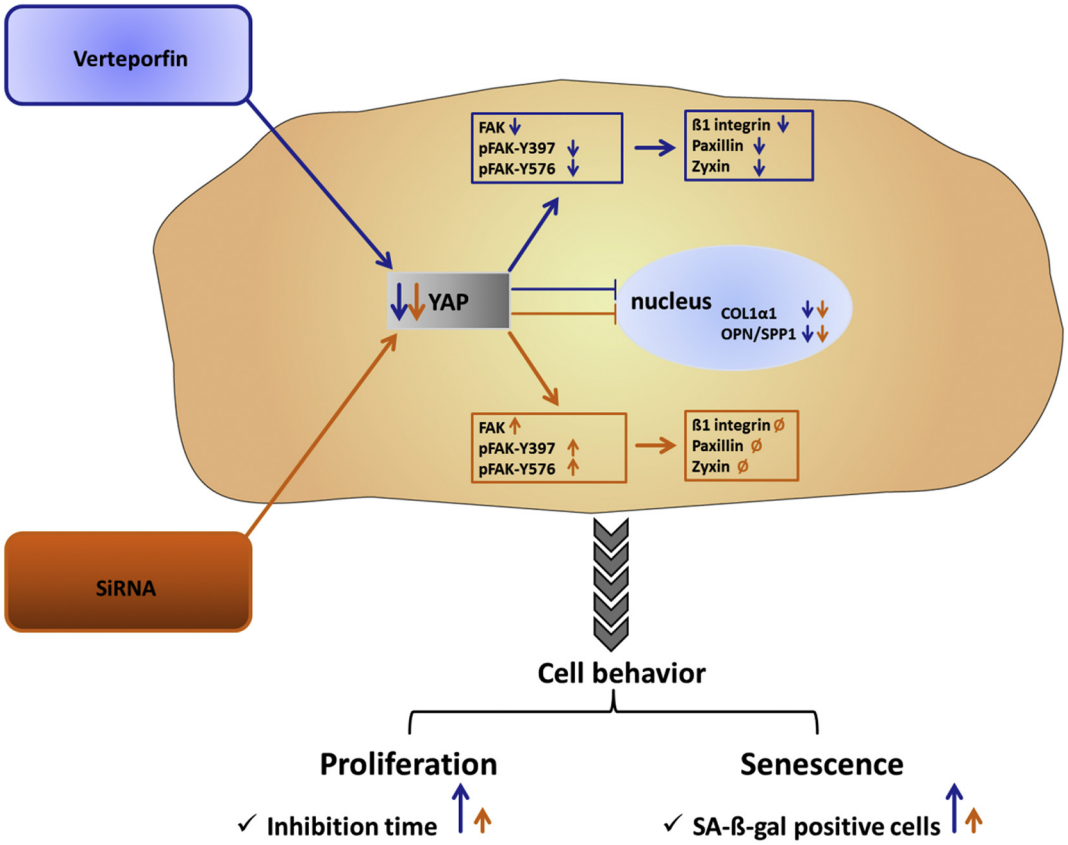

Fig. 7. Consequences of the YAP intervention mode on YAP and FAK as well as hMSC behavior.
VP yields depletion of nuclear YAP, whereby YAP-RNAi decreases the YAP protein in general. Differential effects of VP and RNAi become visible as molecular consequences. With respect to FAK, they are substantiated through FAK down-modulation in conjunction with reduced phosphorylation levels at FAK tyrosine residues 397 and 576, in case of VP. Opposing outcome on FAK and the assessed phosphorylation sites is detected by employing RNAi. Consecutive effects of VP-related impairment of FAK are the re-distribution and concomitant down-regulation of FAs constituents, ß1 integrin, paxillin, and zyxin. These FAs components remain mostly unaffected in case of RNAi. Further approach-independent molecular consequences of YAP intervention include the down-regulation of the osteogenic genes COL1A and SPP1. YAP intervention-triggers consequences on the cell behavioral level become manifest by proliferation decline and senescence increase. While YAP intervention per se induces reduced proliferation, VP extends the inhibition time. Moreover, compared with RNAi, VP causes significant induction of senescence.

transcriptional Yap function in principle requires the activity of the HIPPO pathway-innate kinases LATS1 and LATS2 [25]. Independent of HIPPO regulation, YAP activation has been recently reported to be governed by the cell-circumferential actin belt contraction, which suppresses YAP nuclear localization by involving the Merlin protein [26]. In both cases, the authors have identified HIPPO-independent YAP-regulatory pathways, in which YAP acts as a down-stream effector. However, currently no report is available, which describes molecular consequences on so far identified YAP up-stream targets in the case of YAP intervention. We report here on the inverse way that the employment of two different YAP intervention approaches allows for the analysis of molecular consequences on FAK, thereby pointing to a YAP-FAK-relationship. We found that YAP intervention yielded different outcome on FAK, by strikingly decreasing FAK protein and its activation at the autophosphorylation site FAK^{pTYR397} as well as the kinase activity-indicating site, FAK ^{pTYR576}, in response to VP. In contrast, RNAi led to increased FAK protein and activation levels. These opposing results support the notion that VP, in addition to prevent YAP nuclear localization, directly acts on FAK, although the precise mechanism still has to be clarified. On the other hand, increased FAK protein and its phosphorylation at analyzed sites detected following RNAi-treatment may result from RNA-activation (RNAa), which appears to be conserved in mammalian cells and is triggered by both endogenous and artificially designed small RNAs([27]). RNAa depends on Argonaute proteins, but possesses kinetics distinct from that of RNAi. Epigenetic changes are associated with RNAa and may contribute to transcriptional activation of target genes, but the underlying mechanism remains to be elucidated. In addition, we were able to show that this opposing effect in hMSCs on the YAP-upstream target FAK following application of different YAP-intervention modes, can be found as well in osteosarcoma-derived cells, which point to a generalizable effect of these findings. Employment of the RNAi approach as underlying mechanism of a protein upregulation appears possible, since for instance current studies on breast cancer cell lines proved elevated protein levels of YAP in response to LATS2 kinase-specific siRNA administration [28]. In addition of addressing protein quantities by RNAi, also the activation status of signaling molecules can be affected by preventing transcription of respective cellular genes. This has been exemplified in the case of FAK tyrosine phosphorylation, and here, FAK ^{pTYR397} in particular, by knock-down of the genes LKB1, MARK1, or DXDC1, respectively [10,11]. Taken together, our results deepen the knowledge on YAP, which can be addressed in a HIPPO-independent manner, through its relation to FAK-involving signaling, by first time evidencing the existence of an inverse YAP-FAK-interrelationship. FAK is integral part of the adhesome, which includes the entire network of structural and signaling proteins, involved in regulating cell-matrix adhesion [19,29]. Therefore, it was likely to seek for possible differences of adhesome-inherent constituents, to identify putative molecular implications of the inhibitor-triggered nuclear YAP depletion, as causative of FAK decline. In fact, we could show topological differences for the adhesome components ß1 integrin, paxillin and zyxin, all of them exhibiting a distribution, which was characterized by a less extended topology within

the cytoplasm up to the cell margins. In comparison with the RNAi approach, which yielded fairly similar distribution patterns for the analyzed adhesome constituents with matched controls, inhibitor-treated hMSCs in this regard not only displayed an altered immunolocalization, but also divergent protein quantities, as determined by WB analysis. These findings suggest that YAP intervention, induced by VP, not merely hampers FAK-emerging signaling, as indicated by the reduced levels of FAK ^{pTYR576}, but may also have an impact on FAs architecture. With respect to the YAP-FAK-interrelation, the results show that in dependence of the YAP intervention mode it implies additional molecular consequences, which become apparent on the level of FAs. Such consequences on FAs architecture appear possible, since for instance FAs integrins like ß1 are mandatory to initiate FAK autophosphorylation at ^{pTYR397}, the latter indispensable for FAK clustering, which in turn promotes FAs formation (for review see [30]). In addition, FAK-paxillin interactions have been described to be essential for FAK targeting to FAs [31], and thus FAs establishment. A further evidence of inhibitor-related alterations in FAs integrity is provided by the situation, observed for zyxin in VP-treated hMSCs. Here, the seen alterations may affect the maturation of FAs, since zyxin is established as the most prominent protein marker for mature FAs, which is lacking in nascent adhesions and focal complexes as well (for review see [32]).

With respect to molecular implications, emerging from the loss of YAP, though considering adhesions other than cell-matrix junctions, a brand-new paper, published by Neto et al., has proven defects in lateral cell junctional adherens junctions [33]. In conjunction with our findings, the results described by Neto et al., support the notion of YAP nuclear intervention may address cellular junctions in a more general term.

Regarding our finding that YAP depletion led to the down-regulation of osteogenic gene transcription, it is noteworthy to mention that current studies reveal a connection between the YAP and hMSC osteogenesis. In a study conducted with hMSCs, Dupont and co-workers have demonstrated that on hard substrates, hMSC osteogenic differentiation requires YAP, and that vice versa, depletion of YAP prevents hMSC from adopting the osteogenic phenotype [34]. Based on these results, the down-regulation of COL1A and SPP1, seen in our study, could be a consequence of impairing the function of YAP, which was triggered by pharmacological as well as transcriptional YAP intervention. This hypothesis is backed up by recent findings, elaborated on bone marrow-derived stem cells, which revealed that their osteogenic differentiation is hampered in response to inactivated YAP signaling [35]. On the molecular level, the COL1A and SPP1 down-regulation, observed in this study, may be considered as a general consequence of YAP depletion, since it was detected for both of the chosen YAP-intervention-approaches, irrespective from their impact on FAK. Thus, our YAP-dependent results on COL1 and SPP1 suggest that they may represent candidates of YAP-regulated target genes, and that YAP depletion may per se render a strategy to identify further cellular YAP targets. In this subject matter, also FAK has to be included, since the modulation of transcription is the essential criterion and not whether a gene is up or down-regulated. In our study, YAP intervention led to both, negative, inhibitor (VP)-related, as well as positive, siRNA-linked influence on FAK transcription, thereby emphasizing the relationship between YAP and FAK. As mentioned above, FAK acts as a match-maker of cell senescence. This role is proven through just published studies in senescent hMSCs, where cell senescence could be overcome by the activation of cell-inherent signaling pathways, involving FAK [36]. Due to this decisive role, negative impact on FAK should be assumed to favor this cell behavioral feature, which ends up in cessation of cell growth [24]. Actually, we have detected senescence modulation in both scenarios, employed for YAP depletion. In case of employing YAP RNAi, senescence appeared to be marginally elevated. At first glance, this finding seems to be inconsistent with the aforementioned role of FAK, since FAK has risen, concerning its protein amount and phosphorylation at FAK^{pTYR397} and FAK^{pTYR576} in hMSCs, subjected to RNAi. However, in light of the finding that phosphorylation of FAK is increased in senescent human dermal fibroblasts [37], this seeming inconsistency may be explained. On the other hand, FAK depletion, detected under the regimen of VP caused significant increase of senescence in our hMSCs. These findings fit to the current concepts of the role of FAK within the senescence context, and reveal that in the present study, the YAP-FAK-relationship becomes manifest through this cell behavioral feature.

On the mechanistic level, current studies have shown that the contribution of YAP on proliferation is substantiated by YAP's ability to complex the transcription factor PKNOX1, and within this complex, controls cell cycle-innate S-phase temporal progression [38](for review see [39]). With respect to proliferation, we have detected fairly congruence for both YAP intervention approaches on proliferation inhibition in hMSC cultures. This situation is in line with previously published own findings on VP-related proliferation inhibition [16], and emphasizes the decisive role of YAP in proliferation regulation. Despite the observed congruence in proliferation decline, the time duration needed to slow down proliferation around a cell index of about 0.9 is quite accurately 24 h longer in the VP-treated cells. Based on the findings elaborated for these two facets of cell behavior, i.e. senescence and proliferation, it appears possible that the inhibitor-related extended time duration is associated with FAK. Such an involvement of FAK in the temporally-coupled proliferation inhibition, particularly in case of VP, can be explained by FAK depletion-triggered senescence, since senescence, after having fully established in cells, entails cessation of proliferation. Although both, FAK decrease-induced senescence and YAP depletion affect proliferation, it cannot be excluded that in VP-exposed hMSCs progressive cell-inherent establishment of senescence yields a retardation of proliferation, and is hereby involved in the observed elongated time duration. In case of YAP, its intervention-caused proliferation inhibition may be based on the fostering of the depletion of S-phase traversing cells, an explanatory implication, which may be obtained from the above-cited work of Cabochette et al.

5. Conclusion

Taken together, the co-transcriptional activator YAP is functionally involved in the regulation of fundamental processes such as development, tissue homeostasis, and malignant tumor progression [40].Though YAP is so far considered as a HIPPO pathway effector, there is growing evidence of YAP regulation other than HIPPO, e.g. via FAK signaling. Although studies unraveled the relationship between FAK and YAP, the inverse relation, i.e. the YAP-FAK-interrelationship is so far unknown. In this study, we identified an opposing action of YAP depletion on FAK, which depends on the modus operandi chosen for YAP intervention, while further molecular consequences, including down-regulation of osteogenic genes COL1A and SPP1, were modus-independent. We found diminishment of FAK protein and phosphorylation in case of pharmacological intervention, while FAK was positively stimulated by YAP-RNAi. Moreover, we were able to confirm these opposing results dependent on the mode of YAP-intervention in Saos cells, which point at a generalizable mechanism in cell types of different tissue/− and health status origin. These findings identify that FAK regulation is governed by YAP depletion per se, whereat the outcome of FAK modulation occurs in an operation mode-dependent manner, by either addressing YAP subcellular topology or gene transcription. More importantly, they first time provide evidence for a YAP-FAK-interrelation. On the cell behavioral level, this interrelation involves hMSC proliferation and senescence. Our findings on nuclear YAP intervention may help in tagging further up-stream signaling events and thereby deepen the knowledge of YAP acting as an effector in cell-inherent signaling pathways in general. Moreover, they may open the road to identify further genes, requiring YAP as a co-transcriptional activator.

Authors' contributions

PT and TS designed the conceptual idea of the study, analyzed and interpreted the data. AH performed the experiments. PT, AH and TS wrote the manuscript. MD, BJ, OP and JR critically revised the manuscript. All authors approved the submission of this manuscript in its final form.

Declaration of Competing Interest

The authors declare no potential conflicts of interest with respect to the authorship and/or publication of this article.

Acknowledgements

This joint venture project has been funded by the Deutsche Forschungsgemeinschaft DFG, Germany through grants to Jürgen Rühe and Pascal Tomakidi, Germany. Grant reference number: RU 489/29-1 and TO 198/15-1.

References

[1] F.-X. Yu, B. Zhao, K.-L. Guan, Cell. 163 (2015) 811–828.
[2] Hu JK-H, W. Du, S.J. Shelton, M.C. Oldham, C.M. DiPersio, O.D. Klein, Cell Stem Cell 21 (2017) 91–106. e106.
[3] A. White, J. Khuu, C. Dang, J. Hu, K. Tran, A. Liu, S. Gomez, Z. Zhang, R. Yi, P. Scumpia, Nat. Cell Biol. 16 (2014) 99.
[4] F. Zanconato, G. Battilana, M. Cordenonsi, S. Piccolo, Curr. Opin. Pharmacol. 29 (2016) 26–33.
[5] M.J. LaQuaglia, J.L. Grijalva, K.A. Mueller, A.R. Perez-Atayde, H.B. Kim, G. Sadri-Vakili, K. Vakili, Sci. Rep. 6 (2016) 30238.
[6] A. Elosegui-Artola, I. Andreu, A.E. Beedle, A. Lezamiz, M. Uroz, A.J. Kosmalska, R. Oria, J.Z. Kechagia, P. Rico-Lastres, A.-L. Le Roux, Cell. 171 (2017) 1397–1410. e1314.
[7] C. Wang, X. Zhu, W. Feng, Y. Yu, K. Jeong, W. Guo, Y. Lu, G.B. Mills, Am. J. Cancer Res. vol. 6, (2016) 27.
[8] J.P. Myers, E. Robles, A. Ducharme-Smith, T.M. Gomez, J. Cell Sci. 125 (2012) 2918–2929.
[9] M. Sakabe, J. Fan, Y. Odaka, N. Liu, A. Hassan, X. Duan, P. Stump, L. Byerly, M. Donaldson, J. Hao, Proc. Natl. Acad. Sci. 114 (2017) 10918–10923 201704030.
[10] J. Carretero, T. Shimamura, K. Rikova, A.L. Jackson, M.D. Wilkerson, C.L. Borgman, M.S. Buttarazzi, B.A. Sanofsky, K.L. McNamara, K.A. Brandstetter, Cancer Cell 17 (2010) 547–559.
[11] J.M. Goodwin, R.U. Svensson, H.J. Lou, M.M. Winslow, B.E. Turk, R.J. Shaw, Mol. Cell 55 (2014) 436–450.
[12] Y. Pylayeva, K.M. Gillen, W. Gerald, H.E. Beggs, L.F. Reichardt, F.G. Giancotti, J. Clin. Invest. 119 (2009) 252–266.
[13] T.S. Nowicki, H. Zhao, Z. Darzynkiewicz, A. Moscatello, E. Shin, S. Schantz, R.K. Tiwari, J. Geliebter, Cell Cycle 10 (2011) 100–107.
[14] A. Husari, D. Hülter-Hassler, T. Steinberg, S.D. Schulz, P. Tomakidi, Biochimica et Biophysica Acta (BBA)-Mol Cell Res. 1865 (2018) 209–219.
[15] J.E. Gilda, A.V. Gomes, Anal. Biochem. 440 (2013) 186–188.
[16] D. Hülter-Hassler, M. Wein, S.D. Schulz, S. Proksch, T. Steinberg, B.A. Jung, P. Tomakidi, Exp. Cell Res. 361 (2017) 93–100.
[17] P. Tomakidi, S. Schulz, S. Proksch, W. Weber, T. Steinberg, Cell Tissue Res. 357 (2014) 515–526.
[18] Y.-L. Tai, L.-C. Chen, T.-L. Shen, Biomed. Res. Int. 2015 (2015).
[19] B. Geiger, J.P. Spatz, A.D. Bershadsky, Nat. Rev. Mol. Cell Biol. 10 (2009) 21.
[20] A.J. Engler, S. Sen, H.L. Sweeney, D.E. Discher, Cell. 126 (2006) 677–689.
[21] D.T. Yamaguchi, World J Stem Cells. 6 (2014) 94.
[22] Q. Chen, P. Shou, L. Zhang, C. Xu, C. Zheng, Y. Han, W. Li, Y. Huang, X. Zhang, C. Shao, Stem Cells 32 (2014) 327–337.
[23] U. Ehmer, J. Sage, Mol. Cancer Res. 14 (2016) 127–140.
[24] F. Rodier, J. Campisi, J. Cell Biol. 192 (2011) 547–556 jcb. 201009094.
[25] B. Zhao, L. Li, K. Tumaneng, C.-Y. Wang, K.-L. Guan, Genes Dev. 24 (2010) 72–85.
[26] K.T. Furukawa, K. Yamashita, N. Sakurai, S. Ohno, Cell Rep. 20 (2017) 1435–1447.
[27] V. Portnoy, V. Huang, R.F. Place, L.C. Li, Wiley Interdiscip Rev: RNA. 2 (2011) 748–760.
[28] K. Hua, B. Zhao, J. Jin, H. Xu, C. Wu, D. Li, H. Song, J. Song, J. Zhao, L. Fang, Int. J. Clin. Exp. Pathol. 9 (2016) 2765–2776.
[29] C.A. Whittaker, K.-F. Bergeron, J. Whittle, B.P. Brandhorst, R.D. Burke, R.O. Hynes, Dev. Biol. 300 (2006) 252–266.
[30] M.A. Wozniak, K. Modzelewska, L. Kwong, P.J. Keely, Biochimica et Biophysica Acta (BBA)-Mol Cell Res. 1692 (2004) 103–119.
[31] T.B. Deramaudt, D. Dujardin, F. Noulet, S. Martin, R. Vauchelles, K. Takeda, P. Rondé, PLoS One 9 (2014) e92059.
[32] H. Wolfenson, I. Lavelin, B. Geiger, Dev. Cell 24 (2013) 447–458.
[33] F. Neto, A. Klaus-Bergmann, Y.T. Ong, S. Alt, A.-C. Vion, A. Szymborska, J.R. Carvalho, I. Hollfinger, E. Bartels-Klein, C.A. Franco, eLife. 7 (2018) e31037.
[34] S. Dupont, L. Morsut, M. Aragona, E. Enzo, S. Giulitti, M. Cordenonsi, F. Zanconato, J. Le Digabel, M. Forcato, S. Bicciato, Nature. 474 (2011) 179.
[35] S.-C. Tao, Y.-S. Gao, H.-Y. Zhu, J.-H. Yin, Y.-X. Chen, Y.-L. Zhang, S.-C. Guo, C.-Q. Zhang, Sci. Rep. 6 (2016) 26835.
[36] J.H. Lee, C.W. Yun, J. Hur, S.H. Lee, Marine Drugs. 16 (2018) 121.
[37] H. Zou, E. Stoppani, D. Volonte, F. Galbiati, Mech. Ageing Dev. 132 (2011) 533–542.
[38] P. Cabochette, G. Vega-Lopez, J. Bitard, K. Parain, R. Chemouny, C. Masson, C. Borday, M. Hedderich, K.A. Henningfeld, M. Locker, Elife. 4 (2015).
[39] Z. Meng, T. Moroishi, K.-L. Guan, Genes Dev. 30 (2016) 1–17.
[40] S. Piccolo, S. Dupont, M. Cordenonsi, Physiol. Rev. 94 (2014) 1287–1312.